Attosecond temporal gating with elliptically polarized light

Dudovich, N.; Levesque, J.; Smirnova, Olga; Zeidler, D.; Comtois, D.; Ivanov, M. Yu; Villeneuve, D.; Corkum, Paul

Publisher's version / Version de l'éditeur:
https://doi.org/10.1103/PhysRevLett.97.253903
Physical Review Letters, 97, 25, pp. 253903-1-253903-4, 2006-12-22

Attosecond Temporal Gating with Elliptically Polarized Light

N. Dudovich,[1] J. Levesque,[1,2] O. Smirnova,[1] D. Zeidler,[1,3] D. Comtois,[2] M. Yu. Ivanov,[1] D. M. Villeneuve,[1] and P. B. Corkum[1]

[1]*Steacie Institute for Molecular Sciences, National Research Council of Canada, Ottawa, Ontario K1A 0R6, Canada*
[2]*INRS-EMT, 1650 boulevard Lionel-Boulet, CP 1020, Varennes, Québec J3X 1S2, Canada*
[3]*Carl Zeiss SMT AG, Oberkochen D-73447, Germany*

(Received 14 March 2006; published 22 December 2006)

Temporal gating allows high accuracy time-resolved measurements of a broad range of ultrafast processes. By manipulating the interaction between an atom and an intense laser field, we extend gating into the nonlinear medium in which attosecond optical and electron pulses are generated. Our gate is an amplitude gate induced by ellipticity of the fundamental pulse. The gate modulates the spectrum of the high harmonic emission and we use the measured modulation to characterize the sub-laser-cycle dynamics of the recollision electron wave packet.

DOI: 10.1103/PhysRevLett.97.253903 PACS numbers: 42.65.Ky, 32.80.−t, 42.65.Re

The resolution with which we can measure optical pulses is not limited by the duration of the pulse itself: much higher resolution can be achieved using "optical gating" techniques [1]. One measures a signal proportional to the Fourier transform of the time-dependent signal of interest multiplied by a temporal gate. The temporal resolution is dictated by the response of the observable to a temporal shift of the gate. Current methods of characterizing attosecond pulses with a strong infrared field [2–4] can be viewed as a version of this technique [5].

Attosecond optical pulses arise from electron-ion collision induced by intense optical field. This recollision occurs on the sub-laser-cycle time scale. Attosecond dynamics experiments can use the attosecond optical pulses [6] or the attosecond electron-ion interaction [7,8] for measuring dynamics. We show that gating can be applied directly to the collision process enabling attosecond pulses to be measured as they are produced. This approach can be extended to probe molecular dynamics [7,8], attosecond multielectron [9,10], or nuclear [11] dynamics with much greater resolution.

Recollision occurs when an intense laser field removes an electron from its parent atom (often via tunnel ionization). As the free electron wave packet oscillates in the laser field, it can elastically or inelastically scatter with its parent atom, producing excitation, multiple ionization, or extreme ultraviolet (XUV) radiation. Recollision offers the potential for gating because a perturbation applied to the laser field can slightly modify (gate) the free electron trajectory without modifying the ionization probability or its kinetic energy distribution. Yet, the influence of the perturbation will be imprinted on the generated attosecond pulse, the spectrum of the scattered electron and the spectrum of the correlated products produced by inelastic scattering. Since the recollision can occur within one laser cycle, the applied gate—the perturbation of the electron trajectory—can have a subcycle resolution.

For our gate, we exploit the ellipticity of the field by adding a weak perpendicular component to the fundamental pulse. As the electron moves away from the ion, the additional field shifts the wave packet laterally. The response of the recollision phenomena to ellipticity has been extensively studied in various experiments [12–15]. These experiments utilized the laser ellipticity to measure lateral distribution of the electron wave packet by displacing it laterally. That is, the local interaction between the recollision electron and the ion is a spatial gate. Ellipticity is a mean of translating the gate through the spatial distribution of the electron. We generalize this approach and show that laser ellipticity provides both spatial and temporal information with subcycle resolution.

Ellipticity can form a temporal gate because the induced lateral shift depends nonlinearly on the time of recollision t and the time of ionization (birth) $t_b = t_b(t)$, suppressing different harmonics nonuniformly. Generally, the lateral shift accumulated on short electron trajectories increases with the delay $t - t_b$, and therefore with the harmonic number [see Fig. 1(a)]. The time-dependent response of the electron pulse is determined by measuring the variations in the harmonic spectrum. We emphasize that highly nonlinear processes can be perturbed in other ways. For example, the addition of a weak second harmonic field,

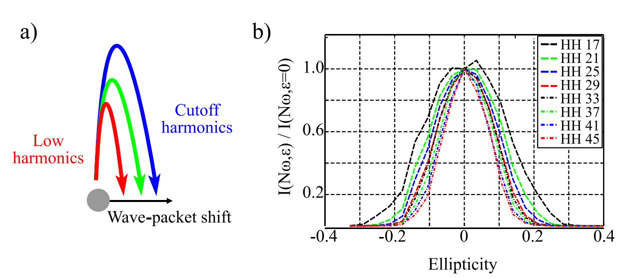

FIG. 1 (color online). (a) Schematic description of the electron wave packet's lateral shift induced by ellipticity for three typical short electron trajectories. (b) Experimentally measured ellipticity response for Ne atoms. Presented are the harmonics yield as a function of the laser ellipticity, normalized to the signal measured with $\epsilon = 0$.

with polarization parallel to the fundamental field, induces a subcycle phase gate [16].

Consider an elliptically polarized laser field: $E = E_0 \cos\omega t \hat{x} + i\epsilon E_0 \sin\omega t \hat{y}$, where $\epsilon \ll 1$ is small ellipticity. Quantum analysis of harmonic generation in elliptical laser field (see, e.g., [13–15]) can be summarized as follows. First, the emission at a moment t comes from those trajectories that return to the parent ion in spite of the lateral shift $\Delta y_L(t, t_b, \epsilon)$ induced by the y component of the field. The return is possible because the electron wave packet emerging in the continuum after tunneling is confined laterally and hence has the corresponding perpendicular velocity distribution. The displacement $\Delta y_L(t, t_b, \epsilon)$ is compensated by the displacement $\Delta y_{v_y}(t, t_b)$ due to the initial perpendicular velocity V_y. The emission intensity follows the probability of having the appropriate initial velocity $V_y = V_y(t, t_b, \epsilon)$ for which $\Delta y_L(t, t_b, \epsilon) = \Delta y_{v_y}(t, t_b)$. The dependence on the initial V_y is Gaussian [17],

$$|\Psi(V_y)|^2 \propto e^{(-V_y^2/V_0^2)}, \tag{1}$$

where V_0, the lateral velocity bandwidth, is assumed to be independent of t_b. Both the Gaussian shape and the independence of V_0 on time have been checked by numerical simulations in Ref. [17] for a two-dimensional soft-core Coulomb potential. Equation (1) also appears in standard analytical tunneling theories, both for the short-range and the Coulomb potential (see, e.g., [17–19]).

We model the lateral dynamics using the classical three-step-model under the strong field approximation (SFA) [20]. That is, we ignore the influence of the Coulomb potential of the ion on the lateral shift of the electron. We discuss this approximation at the end of this Letter and show that it is adequate for perturbative gates. The approximated lateral shift is

$$\Delta y_L(t, t_b, \epsilon) = \frac{\epsilon E_0}{\omega^2}[\cos(\omega t_b)\omega(t - t_b) - \sin\omega t + \sin\omega t_b]. \tag{2}$$

The initial velocity V_y required to ensure $V_y(t - t_b) = \Delta y_L(t, t_b, \epsilon)$ is

$$V_y(t, t_b, \epsilon) = \frac{\epsilon E_0}{\omega}\left[\cos(\omega t_b) - \frac{\sin\omega t - \sin\omega t_b}{\omega(t - t_b)}\right] \equiv \epsilon \tilde{V}(t). \tag{3}$$

In the perturbative regime, the recollision probability is modified as follows:

$$P(t, t_b, \epsilon) = P_0(t)\Gamma(t, t_b, \epsilon) = P_0(t)e^{(-\epsilon^2\tilde{V}^2(t,t_b)/V_0^2)}, \tag{4}$$

where $P_0(t)$ is the unperturbed recollision probability and $\Gamma(t, t_b, \epsilon) = e^{(-\epsilon^2\tilde{V}^2(t,t_b)/V_0^2)}$ serves as a *temporal amplitude gate* induced by ellipticity.

The required initial velocity V_y in Eq. (3) is a time-dependent function. The amplitude gate determined by $V_y(t, t_b)$ changes on a subcycle time scale, at a rate dictated by the width of the initial velocity distribution V_0 and the ellipticity. The electron dynamics can be reconstructed by applying SFA to estimate $\Gamma(t, t_b, \epsilon)$ while treating $P_0(t)$ as an unknown. The SFA is accurate as long as $\epsilon \ll 1$. Gating the relative probability of recollision and therefore characterizing the electron wave-packet dynamics is equivalent to gating the harmonics emission time (unless the recollision electron energy is near a resonance).

We demonstrate gating experimentally by measuring the harmonic spectrum generated from Ne for different ellipticity values and using this information to measure harmonics time of emission. High harmonics were generated with 800 nm, 30 fs laser pulses focused with a 50 cm lens at 2×10^{14} W/cm^2. The harmonics spectrum was measured by an XUV spectrometer.

It is important that the spectral variations result only from lateral displacement of the electron. Therefore, we kept the intensity component in the x axis constant. Keeping E_x constant is especially important for spectral components close to the cutoff energy. This was achieved with a zero order half-wave plate and a polarizer located at the laser output that served as a variable attenuator. We transformed the laser polarization from linear to elliptical using a zero order half-wave plate followed by a quarter-wave plate. Rotating the half-wave plate increases the laser ellipticity continuously, while keeping the major polarization axis in a fixed direction.

Figure 1(b) presents the measured harmonic signal $I(N\omega, \epsilon)$ generated in Ne, as a function of ellipticity. Integrating each harmonic peak, we calculate the spectral response to ellipticity, normalized by the signal measured with linear polarization. The higher harmonic orders are more sensitive to the ellipticity. Thus, small manipulation of the laser polarization not only suppresses the total harmonic yield, but also significantly modifies the spectral distribution. This spectral modification is exploited to resolve the dynamics of the electron wave packet.

While the unperturbed dynamic is unknown, we assume that the relation between t and t_b is given by the classical SFA. The gate therefore becomes a function of a single variable and is expressed as $\Gamma(t, \epsilon)$. Although our gate is a subcycle, for small ϵ the induced gate does not change during the emission window of each particular harmonic within one laser cycle. Therefore, we can write the harmonic response to the ellipticity as

$$I(N\omega, \epsilon) = I(N\omega)\Gamma(t_N, \epsilon) = I(N\omega)e^{(-\epsilon^2\tilde{V}^2(t_N)/V_0^2)}, \tag{5}$$

where t_N is the Nth harmonic emission time. This maps the gate from the time domain onto the frequency domain: $\Gamma(N\omega, \epsilon) = \Gamma(t_N, \epsilon) = I(N\omega, \epsilon)/I(N\omega, \epsilon = 0)$. For small ϵ, Fig. 1(b) presents a direct measurement of $\Gamma(N\omega, \epsilon)$. Now Eq. (4) shows that the temporal information can be recovered by calculating

$$\tilde{V}(N\omega) \equiv \tilde{V}(t_N)/V_0 = \sqrt{-\ln[I(N\omega, \epsilon)/I(N\omega, 0)]}/\epsilon \tag{6}$$

and using the expression for $\tilde{V}(t)$ in Eq. (3) to find t_N.

Figure 2(a) presents $\tilde{V}(N\omega)$ calculated from the measured results, normalized to the maximal value achieved at the cutoff frequency for $\epsilon = 0.11$. With such normalization, the dependence on E_0/V_0 is eliminated and the measured quantity is $\tilde{V}(t_N)/\tilde{V}(t_{N_{\max}})$. Measurements taken for different ellipticity values below $\epsilon = 0.15$ overlap within the experimental error, confirming the perturbative regime and linear dependence of $V_y(t, \epsilon)$ on ϵ. An average response composed of the different measurements is represented by the black line in Fig. 2(a).

Figure 2(b) shows $\tilde{V}(t)/\tilde{V}(t_{N_{\max}})$ calculated from Eq. (3). The required initial velocity increases with the recollision time, reaches its maximum at the $t = 0.65$ cycle (the cutoff harmonic emission time), and then decreases with the time delay. The calculated function represents a *general response* of the electron wave packet to ellipticity, independent of the atomic or molecular structure, laser intensity, or the ionization potential.

Figure 2(a) presents the experimental response, while Fig. 2(b) presents the calculated response. By relating the two we can map each harmonic number to its emission time. We compare the experimental response $\tilde{V}(N\omega)$ to $\tilde{V}(t)/\tilde{V}(t_{N_{\max}})$. By requiring $\tilde{V}(N\omega) = \tilde{V}(t = t_N)/\tilde{V}(t_{N_{\max}})$ we can map the spectral information into the time domain. We calibrated $V(N\omega)$ such that $V(29\omega) = V(t_{29})/V(t_{N_{\max}})$. We choose $V(29\omega)$ since the slope of Fig. 2(b) is large in this frequency range, and therefore the calibration error is minimized. The calibration is equivalent to fixing the time of emission of the 29th harmonic. Figure 2(c) presents the

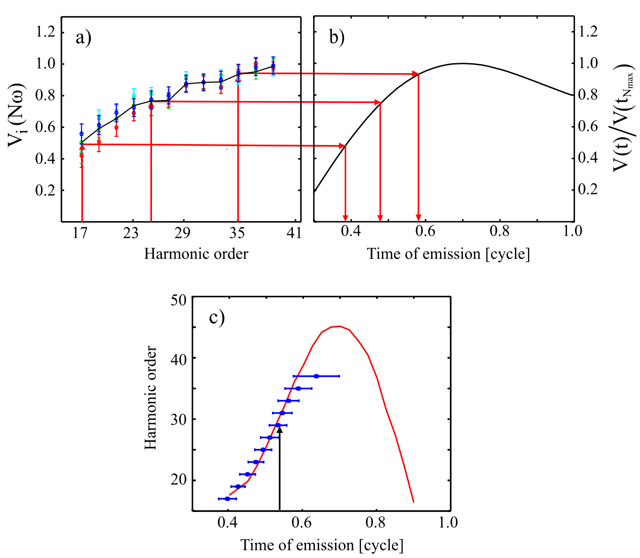

FIG. 2 (color online). Reconstruction of the harmonics time of emission. (a) Initial velocity $\tilde{V}_i(N\omega)$ calculated by Eq. (6) using the experimental response, presented in Fig. 1(b). The experimental measurement and associated errors are presented for the following: $\epsilon = 0.11$ (cyan circles), $\epsilon = 0.14$ (green circles), $\epsilon = -0.11$ (red circles), and $\epsilon = -0.14$ (blue circles). An average response is represented by the black line. (b) Calculated initial velocity $V_i(t)/V(t_{\max})$. (c) Reconstruction of the time of emission for each harmonic number (blue circle) together with the theoretical curve (line). The arrow indicates that we fixed the time of emission of the 29th harmonic.

time of emission of each harmonic that we obtain. Note that although the measurement is performed for the short trajectories, similar analysis can be applied for the long trajectories.

To confirm the validity of our measurement, we cross check our results against a completely different method. The solid curve in Fig. 2(c) shows theoretically calculated times at which different energy components of the recollision electron wave packet return to the ion. It is obtained from a numerical quantum mechanical simulation of the time-dependent Schrödinger equation. The simulation used a 1D soft-core potential with the ionization potential of Ne—21.6 eV. The numerical analysis used window Fourier transform of the returning electron wave packet. The window had both spatial and temporal resolution, provided simultaneously by the 200 asec pulse which probed the recolliding electron by the absorption of one XUV photon. Such absorption is possible only near the core (spatial window); the temporal window was given by the pulse duration. Experimentally reconstructed emission times overlap the theoretical curve within their error bars.

In our analysis so far we have exploited the competition between two weak effects to measure subcycle timing information about the recollision wave packet. The first effect is the constant lateral diffusion of the wave packet from its time of birth until it recollides. The second effect is the time-dependent lateral offset of the wave packet in elliptically polarized light. It may seem that Coulomb focusing is a third weak lateral effect that we have ignored. Before concluding, we show that, for small ϵ, the Coulomb focusing only enters as a higher-order correction.

Using the classical analogue [21] of the quantum approach of Ref. [22], the correction ΔV_y to the velocity V_y is calculated by integrating the Coulomb force along the electron trajectory in the laser field alone. This analysis will naturally allow us to divide the continuum into two regions. The first region is near the core, where the Coulomb force is significant. The second region is far from the core, where the Coulomb force is negligible. We will now show that (i) $\Delta y_L(t, \epsilon)$, $\Delta y_{V_y}(t)$ and their dependence on t are dominated by the second region, and that (ii) $\Delta V_y \ll V_y$.

For the laser field with main polarization along the x axis, the electron emerges at a position $x_i = I_P/E_0$, $y = z = 0$ and is accelerated away by the electric field. In the limit $\alpha \gg x_i$, where $\alpha = E_0/\omega^2$ is the electron oscillation amplitude, the Coulomb integral is accumulated at short times $\tau \ll 1/\omega$ after ionization. This allows us to use the quasistatic approximation for the electron motion near the core, freezing the electric field at the moment of birth t_b, $E_x = E_0 \cos(\omega t_b)$. The correction to V_y is

$$\Delta V_y \approx \int_0 \frac{y(\tau)d\tau}{[x^2(\tau) + y^2(\tau)]^{3/2}} \approx \int_0 \frac{V_y \tau d\tau}{[(x_i + E_x \tau^2/2)^2 + V_y^2 \tau^2]^{3/2}}, \quad (7)$$

where higher-order correction due to the weak y component of the field is neglected. Equation (7) yields

$$\frac{\Delta V_y}{V_y} \approx \frac{1}{2x_i^2 E_x} \frac{1}{1 + V_y^2/(2E_x x_i)} \approx \frac{E_x}{2I_p^2} \frac{1}{1 + V_y^2/(2I_p)}, \quad (8)$$

where we have used the quasistatic relationship $x_i E \approx I_p$. For our experimental conditions, the Coulomb correction is very small: $\Delta V_y / V_y \leq 0.06$. Moreover, since $\Delta V_y \propto V_y$, its dependence in time is no steeper than that of V_y; therefore its contribution to the gate slope is negligible.

The integral in the calculation of ΔV_y is accumulated at $\tau \sim \sqrt{x_i/E_x} \approx \sqrt{I_p}/E_x$ after ionization, while the electron is still close to the core. Ellipticity-induced displacement during this time is $\delta y \sim \epsilon E_x \tau^2/2 = \epsilon \alpha \gamma^2/4$, where γ is the Keldysh parameter. In the regime $\gamma^2 \ll 1$ this displacement is negligible compared to the displacement $\sim \epsilon \alpha_{\mathrm{osc}}$ accumulated far away from the core.

This discussion emphasizes an important property of using weak perturbation for the gate. A perturbative gate can be described with a simple model where Coulomb corrections to the gate are of higher order. Therefore, the ellipticity dependence of high harmonic emission can serve as a simple temporal amplitude gate, which can be modeled by SFA.

We would like to discuss one final issue before concluding. In our analysis we have assumed that the relation between t and t_b is described by SFA. As it stands, the reconstruction procedure represents a self-consistency check of the SFA model. The deviation from the theoretical curve is a two-dimensional function expressed as $\delta V(t_N, t_{bN}) = V(t_N, t_{bN}) - V^{\mathrm{SFA}}$, where $t_N = t_N^{\mathrm{SFA}} + \Delta t_N$ and $t_{bN} = t_{bN}^{\mathrm{SFA}} + \Delta t_{bN}$. Since the measured deviation is a one-dimensional function $\delta V(N\omega)$, there is insufficient information to determine both Δt_N and Δt_{bN}. That is, an unknown correction cannot be unambiguously retrieved within the simple reconstruction procedure used in this Letter.

However, by exploiting the ellipticity data, it is possible to modify the reconstruction procedure to retrieve the unknown dynamics which will manifest itself as deviations from SFA-predicted moments t_N^{SFA} and t_{bN}^{SFA}. We can assume that the small deviations Δt_N and Δt_{bN}, as a function of the harmonic number N, can be approximated with a Taylor expansion in powers of $(N - N_0)$ around some central harmonic N_0 in the plateau region. This assumption significantly reduces the number of free parameters. The few unknown coefficients in the expansion can then be retrieved from a global fit to the ellipticity dependence of the entire harmonic spectrum. Since in our experiment the experimental error bars are larger than the deviation, such a reconstruction cannot be applied.

A closely related alternative approach is to use a movable gate created by a weak second harmonic field polarized perpendicular to the fundamental field. Summed, the fields produce a "subcycle time-dependent ellipticity"—also an amplitude gate. By controlling the phase between the fields we can shift the ellipticity within the laser cycle, making a narrower and much more controllable gate. This gate is a two-dimensional function which allows one to extract both t_N and t_{bN} independently.

Gating techniques can be applied to other high-order nonlinear phenomena. Many people have studied the ellipticity dependence of recollision phenomena. All such data contain previously hidden temporal information [23]. For example, it should be possible to time resolve nonsequential double (or multiple) ionization (or its nuclear equivalent) using gating techniques. If so, then the power of optical gating technology will have been transferred to one important aspect of collision physics—a science where time-resolved measurements are rare.

We acknowledge partial financial support by the National Research Council of Canada, the Rothschild Foundation, the Alexander von Humboldt Foundation, the Canadian Institute for Photonic Innovation, NSERC Accelerator grant program, and NSERC Special Research Opportunities grant program.

[1] D. J. Kane and R. Trebino, IEEE J. Quantum Electron. **29**, 571 (1993).
[2] M. Hentschel *et al.*, Nature (London) **414**, 509 (2001).
[3] J. Itatani *et al.*, Phys. Rev. Lett. **88**, 173903 (2002).
[4] Y. Mairesse *et al.*, Science **302**, 1540 (2003).
[5] F. Quéré *et al.*, J. Mod. Opt. **52**, 339 (2005).
[6] M. Drescher *et al.*, Nature (London) **419**, 803 (2002).
[7] H. Niikura *et al.*, Nature (London) **421**, 826 (2003).
[8] X. M. Tong, Z. X. Zhao, and C. D. Lin, Phys. Rev. Lett. **91**, 233203 (2003).
[9] M. Weckenbrock *et al.*, Phys. Rev. Lett. **92**, 213002 (2004).
[10] A. Rudenko *et al.*, Phys. Rev. Lett. **93**, 253001 (2004).
[11] N. Milosevic, P. B. Corkum, and T. Brabec, Phys. Rev. Lett. **92**, 013002 (2004).
[12] K. S. Budil *et al.*, Phys. Rev. A **48**, R3437 (1993).
[13] P. Dietrich *et al.*, Phys. Rev. A **50**, R3585 (1994).
[14] N. H. Burnett, C. Kan, and P. B. Corkum, Phys. Rev. A **51**, R3418 (1995).
[15] P. Antoine *et al.*, Phys. Rev. A **53**, 1725 (1996).
[16] N. Dudovich *et al.*, Nature Phys. **2**, 781 (2006).
[17] M. Y. Ivanov *et al.*, J. Mod. Opt. **52**, 165 (2005).
[18] V. S. Popov, Usp. Fiz. Nauk **174**, 921 (2004) [Sov. Phys. Usp. **47**, 855 (2004)].
[19] N. B. Delone and V. P. Krainov, *Multiphoton Processes in Atoms* (Springer, New York, 1994).
[20] P. B. Corkum, Phys. Rev. Lett. **71**, 1994 (1993).
[21] S. P. Goreslavski *et al.*, Phys. Rev. Lett. **93**, 233002 (2004).
[22] O. Smirnova, M. Spanner, and M. Ivanov, J. Phys. B **39**, S307 (2006).
[23] G. G. Paulus *et al.*, Phys. Rev. Lett. **80**, 484 (1998).